

130°K, where the elastic moduli reveal the "intermediate" range anomalies (from 125 to 96°K).

Figure 2 shows the variation of the Debye temperature Θ_D with temperature. At 0°K, $\Theta_D=485^\circ\text{K}$, a value significantly higher than those obtained from specific-heat (376°K)^{2,3} and x-ray measurements (390°K).¹⁵ Weiss *et al.*¹⁵ separated the magnetic part of the specific heat and tried to correlate the magnetic

¹⁵ C. P. Gazzara, R. M. Middleton, and R. J. Weiss, *Phys. Letters* **10**, 257 (1964).

entropy with the spins by a well-established relation.¹⁶ Adopting $\Theta_D=390^\circ\text{K}$ the agreement was poor; but our value of 485°K would confirm the validity of this relation in $\alpha\text{-Mn}$.

The author would like to acknowledge the benefit of stimulating discussions with Professor S. Shtrikman of the Weizmann Institute of Science, Rehovoth, and with Dr. G. Erez, N.R.C.N., Beer-Sheva.

¹⁶ J. A. Hofmann, A. Paskin, K. J. Taner, and R. J. Weiss, *J. Phys. Chem. Solids* **1**, 45 (1956).

Lattice Vibrations of Solid Solutions; Infrared Absorption Spectra of Nitrate Ions in Alkali Halides

R. METSELAAR* AND J. VAN DER ELSKEN

Laboratory for Physical Chemistry, University of Amsterdam, Amsterdam, The Netherlands

(Received 26 June 1967)

Infrared-absorption spectra of alkali halide single crystals with nitrate-ion impurities show a fine structure on the internal vibrational bands of the nitrate ion that must be ascribed to combinations with the lattice modes of the crystal. A part of these combinations arises from lattice modes that are practically the same as for the unperturbed lattice. Specific heats calculated from the observed spectra are in excellent agreement with the calorimetrically determined values for the pure alkali halide crystals. Other features in the experimentally obtained spectra must be ascribed to combinations with local modes. Group-theoretical considerations lead to selection rules for first-order transitions involving these lattice modes, as well as for absorption due to combinations with the internal vibrational or electronic transitions. A model calculation gives the frequencies of the local modes in terms of the eigenvectors and eigenfrequencies of the unperturbed lattice with the ratio of the masses of the substituted ion and the impurity ion as parameter. Calculated local-mode frequencies are compared with the observed frequencies and with frequencies that have been reported in the literature.

I. INTRODUCTION

THE study of the interactions governing the behavior of solids by means of infrared-absorption spectroscopy is not limited to the classical measurements of the optically active lattice modes of the crystals in the far infrared, but can be extended to the measurements of the active internal vibrations of the ions or molecules constituting the crystal. Important information about the crystal may be obtained, when consideration is given to the shapes and fine structures of the absorption features. On theoretical grounds we may distinguish three types of interactions which will influence the shape and structure of the absorption bands. First, there is a static effect, which can be described as a perturbation of the potential-energy function of the free molecule or ion due to the field of the surrounding lattice in its equilibrium configuration. Several authors have reported on the influence of this perturbation on the positions and the degeneracies of the vibrational and rotational levels.¹ The second type

* Present address: Philips Research Laboratory, N. V. Philips' Gloeilampenfabrieken, Eindhoven, The Netherlands.

¹ L. Pauling, *Phys. Rev.* **36**, 430 (1930); A. F. Devonshire, *Proc. Roy. Soc. (London)* **A153**, 601 (1936); A. Maki and J. C. Decius, *J. Chem. Phys.* **31**, 772 (1959); W. Vedder and D. F. Hornig, *ibid.* **35**, 1560 (1961).

of interaction is the dynamic coupling of the internal vibrations of different ions or molecules, which may have a profound influence on the appearance of the absorption spectrum.² The third type of interaction is that between the displacement coordinates of the complex ion or molecule and the coordinates describing the vibrations of the lattice. This interaction has been neglected by most investigators, since it is expected to be small with regard to the above mentioned perturbations. One may hope, however, that under suitable conditions this interaction will afford some insight into the lattice dynamics of the crystals. The coupling between an internal vibration and a lattice mode can, in the anharmonic approximation, lead to a combination band in the infrared spectrum. The density of the lattice vibrations is so high, that in spite of the fact that the frequencies are discrete, no sharp bands are expected to occur. As suggested by Mitra,³ it is more likely that broad bands will be observed with an intensity distribution related to the frequency distribution of the lattice modes. Deviations from such a distribution will arise when certain combinations are forbidden

² J. C. Decius, *J. Chem. Phys.* **23**, 1290 (1955).

³ S. Mitra, *J. Chem. Phys.* **39**, 3031 (1963).

TABLE I. Peak extinction coefficients for NO_3^- and NO_2^- in KBr; room-temperature values.

Frequency (cm^{-1}) ϵ_{max} (cm^2/mM)	KBr: NO_3^-		$\nu_1 + \nu_4$	$\nu_1 + \nu_3$	$2\nu_3$	KBr: NO_2^- $2\nu_3$
	ν_2	ν_3				
	838	1387	1766	2426	2764	2556
	129	2×10^4	32	132	24	54

for reasons of symmetry. Systems in which one may expect to be able to discern these weak combination bands are formed by dilute solid solutions of complex ions in alkali-halide single crystals. The dynamic coupling effects are not operative in these systems as long as the concentration of the complex ions is kept low enough to avoid clustering of the ions.⁴ It will be preferable then to choose an ion with a strong fundamental vibration band and to use samples with long path lengths. The latter condition can be fulfilled by growing large single crystals of the alkali halides from the melt. From the few existing ions which can be substituted in single crystals in this way, the nitrate ion is among the most favorable, having a very strong fundamental vibration band ν_3 .

II. EXPERIMENTAL

Single crystals of the alkali halides doped with nitrate or nitrite were grown from the molten salts. The resulting crystals always contain both nitrate and nitrite ions in comparable concentrations.

The lengths of the crystals used in our experiments varied from 8 to 80 mm, with nitrate concentrations in the range from 10^{18} to 10^{17} per cm^3 .

Apart from NO_3^- and NO_2^- , the only impurity ions detectable from the infrared spectrum were trace amounts of NCO^- . For a number of crystals the NO_3^-

and NO_2^- concentrations were determined by means of a spectrophotometric method.⁵ Values of peak extinction coefficients as defined by

$$\epsilon_{\sigma} = (1/cl) \ln(I_0/I)_{\sigma}$$

are shown in Table I.

It was found that the crystals were reasonably homogeneous in the NO_3^- and NO_2^- concentrations, although with a slight increasing concentration from top (first crystallized part) to bottom.

The cells used for our infrared measurements were the conventional type conduction cryostats cooled with liquid nitrogen or liquid helium.

The spectra were measured on Perkin-Elmer models 13 U, 337 and 112 G, flushed with dry nitrogen to remove atmospheric water vapor.

We studied the frequency region near the ν_3 fundamental vibration of the NO_3^- ion in the alkali halides.

Figure 1 gives the absorption spectrum at two different temperatures of a KBr crystal containing both NO_3^- and NO_2^- ions.

At room temperature there are two very broad absorption bands in the region of 1200–1600 cm^{-1} . Cooling with liquid nitrogen (77°K) reveals more structure. The ν_3 and ν_1 fundamentals of nitrite are found at 1280 and 1320 cm^{-1} , respectively. At approximately 1390 cm^{-1} the ν_3 fundamental of nitrate is observed,

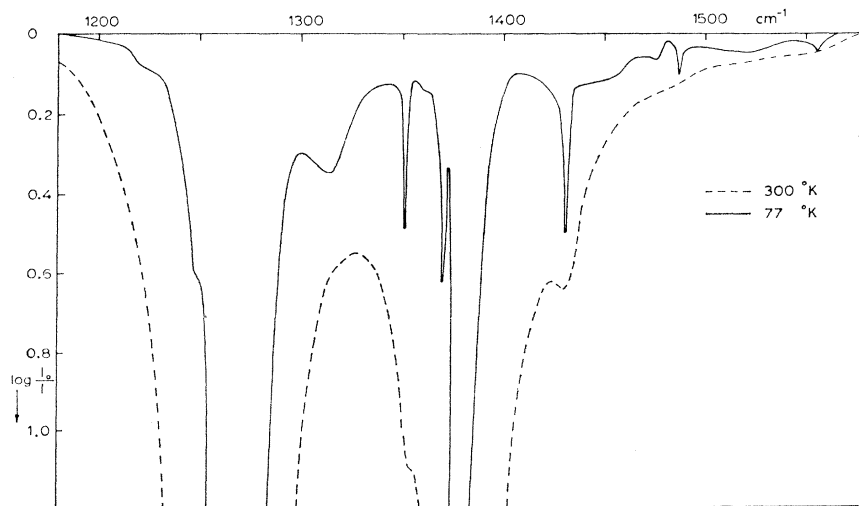


FIG. 1. The frequency region of 1200–1600 cm^{-1} of a KBr crystal containing nitrate and nitrite ions. Crystal thickness 55 mm. $C_{\text{NO}_3^-} = 5.5 \mu\text{M}/\text{cm}^3$, $C_{\text{NO}_2^-} = 8 \mu\text{M}/\text{cm}^3$. Logarithms are to base 10.

⁴ J. van der Elsken and S. G. Kroon, *J. Chem. Phys.* **41**, 3451 (1964).

⁵ W. Gomes, *Z. Anal. Chem.* **216**, 387 (1966).

with a much weaker band at 1430 cm^{-1} , due to the first overtone $2\nu_4$ of nitrate.

We will concentrate our attention here on the absorption structure on the high-frequency side of the nitrate fundamental. This sideband structure is clearly exhibited in the spectrum at 77°K , and remains unaltered in the temperature region $90\text{--}4^\circ\text{K}$; above 90°K the bands broaden rapidly.

Drastic changes are observed in the nitrate ν_3 absorption band itself when the temperature is lowered from 77°K to liquid-helium temperatures. An example is given in Fig. 2, for $\text{KBr}:\text{NO}_3^-$. This high resolution spectrum (spectral slit width $\approx 0.5\text{ cm}^{-1}$), shows a number of very sharp peaks at a few wave-numbers distance from one another. The fine structure is com-

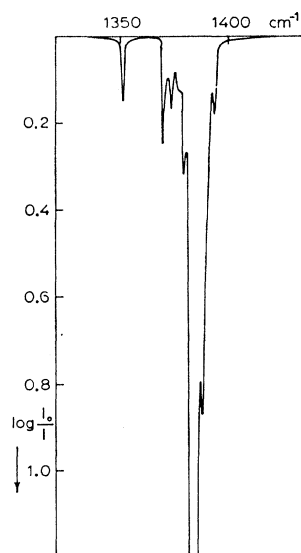


FIG. 2. The ν_3 fundamental of nitrate ions in a KBr crystal cooled with liquid helium. Crystal thickness 9 mm.

$$C_{\text{NO}_3^-} = 5\ \mu\text{M}/\text{cm}^2.$$

Logarithms are to base 10.

pletely spread out at 77°K . It is obvious from the different temperature behavior that the splitting in the main band and the above mentioned sideband structure are of different nature.

The splitting shown in Fig. 2 has been explained as a rotational structure.^{6,7} From the spectra it has been inferred that the nitrate ion might perform a librational motion around the top axis.

At this point we will not discuss the fine structure of the main absorption band; we will concentrate our attention on the sideband structure observed in combination with the nitrate ν_3 . This structure consists of

TABLE II. Frequencies (cm^{-1}) of absorption bands in alkali halides at 77°K relative to the frequency of the ν_3 fundamental vibration band of NO_3^- .

	Approximate maxima of broad bands	Maxima of sharp bands
KI	55	73
	110	87
	135	
KBr	65	95
	85	165
	123	
	133	
KCl	90	...
	115	
	150	
NaI	60	86
	140	
NaBr	65	95
	165	105
	203	113
		128
		221
NaCl	35	...

a continuous absorption with some broad maxima, and extends to about 200 cm^{-1} above the fundamental band. In the alkali bromides and iodides there are also a few sharp bands in this region. A survey of the spectra obtained for a number of alkali halides is given in Fig. 3, while the frequencies of the broad and sharp absorption features are given relative to the nitrate ν_3 frequency in Table II. The frequency of this fundamental in various matrices is shown in Table III.

The dashed lines in Fig. 3 indicate the estimated total contribution of the absorption bands ν_1 of NO_2^- and ν_3 and $2\nu_4$ of NO_3^- to the absorption spectrum shown. We did not obtain reliable results for $\text{NaCl}:\text{NO}_3^-$ because of a clustering of the nitrate ions at the concentrations used (0.01%).

III. GROUP-THEORETICAL CONSIDERATIONS

In order to determine qualitatively whether it is possible to interpret the observed sideband structure in terms of phonon spectra, we can use the rules of group theory.

TABLE III. Frequencies of the ν_3 fundamental vibration of NO_3^- in alkali halides (in cm^{-1}).

KCl	1398	NaCl	1423
KBr	1387	NaBr	1398
KI	1372	NaI	1391

⁶ V. Narayanamurti, W. D. Seward, and R. O. Pohl, Phys. Rev. **148**, 481 (1966).

⁷ R. Bonn, R. Metselaar, and J. van der Elsken, J. Chem. Phys. **46**, 1988 (1967).

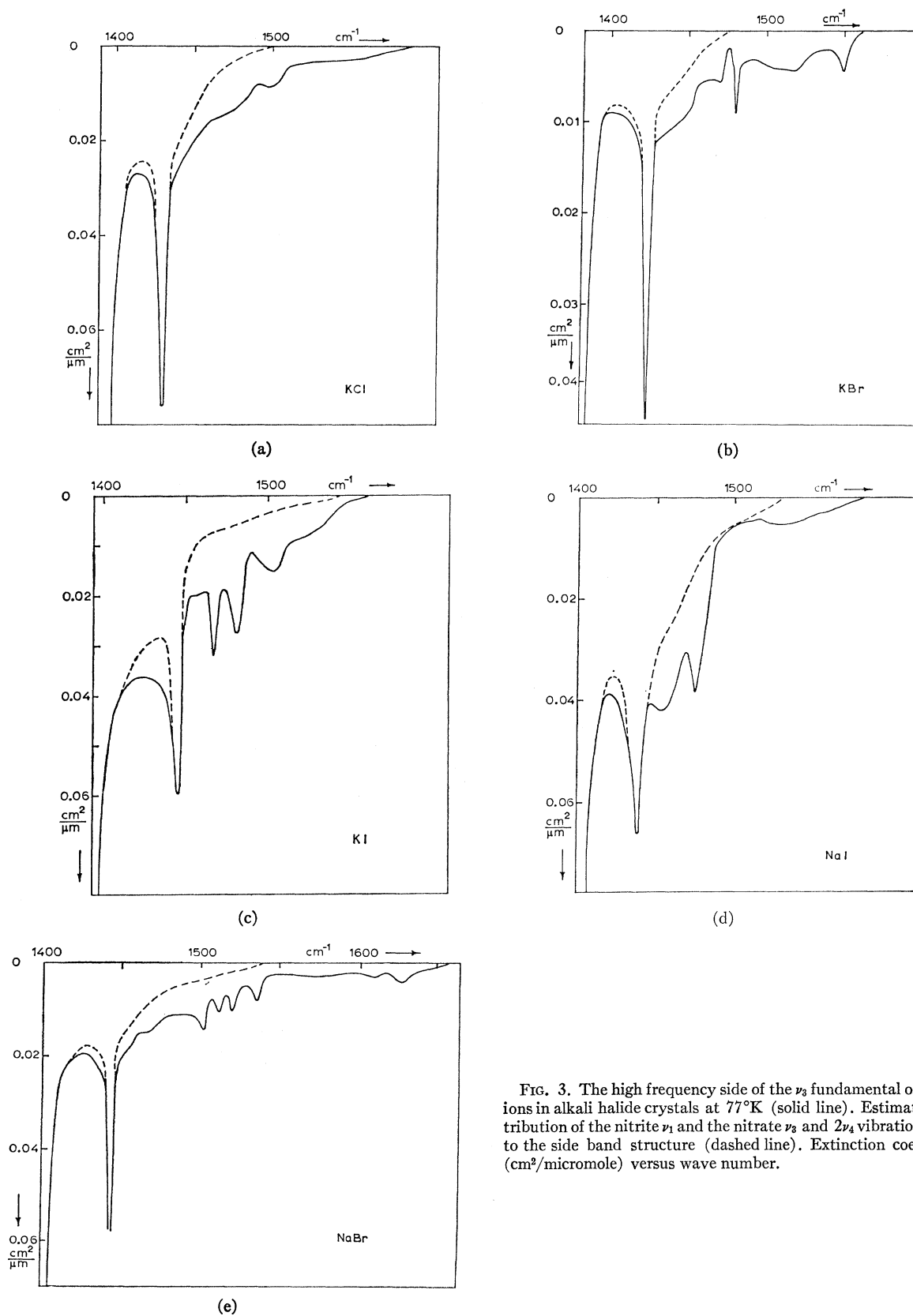


FIG. 3. The high frequency side of the ν_3 fundamental of nitrate ions in alkali halide crystals at 77°K (solid line). Estimated contribution of the nitrite ν_1 and the nitrate ν_3 and $2\nu_4$ vibration bands to the side band structure (dashed line). Extinction coefficients ($\text{cm}^2/\text{micromole}$) versus wave number.

In the perfect lattice, the translational invariance imposes a very strict selection rule, which forbids nearly all phonon transitions. We are, however, interested in the case of dilute solid solutions, which means that one of the ions of the host lattice is replaced by a guest ion, (which will further be designated as "the impurity"). The lattice is now no longer invariant with respect to translations, so the selection rule will be altered too. In general one can say that, when the symmetry at the impurity site is lowered further, more phonon transitions will be allowed.

It should be possible to derive the optical selection rules for the transitions between the energy levels of the complex ion and those of the ions of the host lattice once the local symmetry around the complex ion (and the corresponding character table) is known. The starting points for such a discussion are the space group of the matrix and the point group of the free ion.

For the alkali halides that we used, the space group is $O_h^5 [F(4/m)\bar{3}(2/m)]$, a face-centered cubic group. The lattice can be considered as being built up out of two fcc lattices which are shifted with respect to each other along a half cube diagonal. The character tables for this group have been calculated by Bouckaert, Smoluchowski and Wigner.⁸ All of the different wave vectors \mathbf{k} can be represented by vectors drawn in the symmetrical unit cell in the reciprocal lattice, known as the first Brillouin zone. Figure 4 shows this cell with a number of the most important points in our lattice.

There are six possible vibrational modes for a given wave vector in the Brillouin zone. The characters for each of these six phonons can be obtained by investigating the transformation properties of the corresponding phonon eigenvectors.⁹

Using the eigenvectors for KI from Karo and Hardy's deformation dipole model,¹⁰ we obtained the results shown in Table IV (using the notation of Wilson, Decius, Cross¹¹).

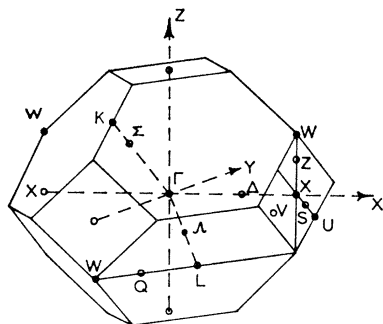


FIG. 4. First Brillouin zone of a face centered cubic lattice.

⁸ L. P. Bouckaert, R. Smoluchowski, and E. Wigner, *Phys. Rev.* **50**, 58 (1936).

⁹ R. Loudon, *Proc. Phys. Soc. (London)* **84**, 379 (1964).

¹⁰ A. M. Karo and J. R. Hardy, *Phys. Rev.* **129**, 2024 (1963).

¹¹ E. B. Wilson, J. C. Decius, and P. C. Cross, *Molecular Vibrations* (McGraw-Hill Book Co., Inc., New York, 1955).

TABLE IV. Phonon symmetries for KI at different points in the Brillouin zone, with respect to K^+ and I^- sites.

K^+ site	Optical branches	Acoustic branches
$L(D_{3d})$	$A_{2u}(LO) + E_u(TO)$	$A_{1g}(LA) + E_g(TA)$
$W(D_{2d})$	$B_2 + E$	$A_1 + E$
$Z(C_{2v})$	$A_1 + B_1 + B_2$	$A_1 + B_1 + B_2$
$\Delta(C_{4v})$	$A_1(LO) + E(TO)$	$A_1(LA) + E(TA)$
$\Lambda(C_{3v})$	$A_1(LO) + E(TO)$	$A_1(LA) + E(TA)$
$\Sigma(C_{2v})$	$A_1 + B_1 + B_2$	$A_1 + B_1 + B_2$
$S(C_{2v})$	$A_1 + B_1 + B_2$	$A_1 + B_1 + B_2$
$X(D_{3h})$	$A_{2u}(LO) + E_u(TO)$	$A_{2u}(LA) + E_u(TA)$
$Q(C_2)$	$A + 2B$	$2A + B$
$\Gamma(O_h)$	F_{1u}	F_{1u}
I^- site	Optical branches	Acoustic branches
$L(D_{3d})$	$A_{1g}(LO) + E_g(TO)$	$A_{2u}(LA) + E_u(TA)$
$W(D_{2d})$	$A_1 + E$	$B_2 + E$
$Z(C_{2v})$	$A_1 + B_1 + B_2$	$A_1 + B_1 + B_2$
$\Delta(C_{4v})$	$A_1(LO) + E(TO)$	$A_1(LA) + E(TA)$
$\Lambda(C_{3v})$	$A_1(LO) + E(TO)$	$A_1(LA) + E(TA)$
$\Sigma(C_{2v})$	$A_1 + B_1 + B_2$	$A_1 + B_1 + B_2$
$S(C_{2v})$	$A_1 + B_1 + B_2$	$A_1 + B_1 + B_2$
$X(D_{3h})$	$A_{2u}(LO) + E_u(TO)$	$A_{2u}(LO) + E_u(TO)$
$Q(C_2)$	$2A + B$	$A + 2B$
$\Gamma(O_h)$	F_{1u}	F_{1u}

Actually, we have to reduce the space-group representations into irreducible representations of the local symmetry group L of the impurity ion. This local symmetry group is defined by all symmetry operations that leave the impurity ion invariant. For the cases discussed here, where a halide ion is replaced by a complex ion, the group L is necessarily a subgroup of the group of the complex ion and a site group of the host lattice.

For NO_3^- the point group of the ion is D_{3h} . Under this group the fundamental vibrations are $\nu_1(a_1')$, $\nu_2(a_2'')$, $\nu_3(e')$ and $\nu_4(e')$, of which the totally symmetric ν_1 is infrared-forbidden, and the others are active. For a substitutional impurity in the most symmetrical position the site group is O_h . In this case the local symmetry group must be a subgroup of O_h and D_{3h} .

The possibilities for L then are D_3 and its subgroups C_{3v} , C_3 , C_2 , C_s or E . In our spectra we always observe a sharp, weak absorption band at 1050 cm^{-1} , attributed to the ν_1 fundamental. As this vibration is still strictly forbidden under the group D_3 , this possibility can be ruled out.

Under the groups C_2 , C_s , or E , the degeneracy of ν_3 and ν_4 would be removed. As no splitting of ν_4 is observed, the groups C_{3v} and C_3 are probable, although the lower symmetry groups cannot be ruled out. This leaves us with the possible local symmetry groups C_{3v} , C_3 , C_2 , C_s , or E . A C_{3v} symmetry means that the threefold axis of the ion is parallel to the cube diagonal of the unit cell while each oxygen atom is equidistant from its two nearest alkali neighbors. That this situa-

TABLE V. Impurity induced infrared activity under the local symmetry groups. Notation of the lattice modes $\nu(\mathbf{k})$ according to Table IV.

Ion	Mol. group	Loc. group	Fundamentals ν_i	Far-infrared phonons $\nu(\vec{k})$	Near-infrared comb. modes $\nu_i + \nu(\vec{k})$
NO_3^-	D_{3h}	C_{3v}	Active for $i=1, 2, 3, 4$	Active for all \mathbf{k}	Active for all i and \mathbf{k}
NO_2^-	C_{2v}	C_{2v}	Active for $i=1, 2, 3$	Active for all \mathbf{k}	Active for all i and \mathbf{k}
N_3^-	$D_{\infty h}$	D_{3d}	Active for $i=2, 3$	$\nu(L)$ LO and TO forbidden; all other phonons active	$\nu_1 + \nu(L)$ LO and TO forbidden; $\nu_2 + \nu(\Gamma)$ forbidden; $\nu_2 + \nu(X)$ forbidden; $\nu_2 + \nu(L)$ LA and TA forbidden; $\nu_3 + \nu(\mathbf{k})$ selection rules equal to those for $\nu_2 + \nu(\mathbf{k})$; all other combinations active
NCO^-	$C_{\infty v}$	C_{3v}	Active for $i=1, 2, 3$	Active for all \mathbf{k}	Active for all i and \mathbf{k}
OH^-	$C_{\infty v}$	C_{4v}	Active	Active for all \mathbf{k}	Active for all \mathbf{k}

tion should be possible has been put forward by Frevel¹² for the case of a nitrate ion in KBr.

For these reasons we have taken group C_{3v} to be the local symmetry group.

The most probable symmetry groups L for a number of different ions are given in Table V.

A reduction of the phonon representations into irreducible representations of the group L allows the investigation of the infrared optical activity of the phonons. The condition for an optically allowed phonon transition is that the 3-dimensional translation vector is contained in the representations of the phonon which is under consideration.

If the representations of the internal vibrations of the complex ion are also known under L , we can find out whether combinations of an internal mode with a lattice mode are allowed.

The results for a number of ions are shown in Table V.

Table V shows clearly that, for a crystal with an impurity, hardly any phonon transition will generally be forbidden for symmetry reasons. Of course the group-theoretical discussion merely informs us whether the transition integrals are zero or nonzero. Only an exact calculation of the matrix elements can give us information about the intensity of the absorption bands.

Such a calculation has been carried out for the phonon absorption due to an impurity in the center of a diatomic linear chain¹³: The extinction coefficients were calculated from an approximation of the dipole moment derivative of the vibrating chain as a function of the mass and the nearest neighbor force constants of the impurity. A very considerable alteration in the intensity distribution over the branches results, de-

pending on the mass and force constant ratio. This implies that the absorption is proportional to the density of states multiplied by a frequency-dependent weight factor. Only in some special cases is this weight factor constant over the whole frequency range.

In our case of a combination band (internal vibration-phonon) the transition is forbidden in the harmonic approximation. The nonzero part of the transition-matrix elements is due to third- and higher-order terms in the dipole-moment expansion. Neither of these contributions is generally known.

If the anharmonic terms are small, perturbation theory can be used for the evaluation of the matrix elements. The denominator of the resulting expression will in that case contain the difference of the frequency of the sideband and the frequency of the main band. This gives a contribution to the weight factor, which causes a decrease in the absorption intensity with increasing distance to the main band (the pure internal transition of the impurity).

However, specific interactions of the impurity with its surroundings can have a more pronounced effect on the weight factor.

This may result in large differences in the absorption spectra, as is clearly demonstrated when we compare two recent publications on the sidebands of localized vibrations of hydrogen ions.

In the case of hydrogen ions in CaF_2 , a decreasing weight factor with increasing frequency difference to the main band was found.¹⁴

On the other hand, the observed sideband structure found with H^- ions in KBr showed that there is mainly coupling to optical phonons in this case. The spectra were satisfactorily explained with a model in which

¹² L. K. Frevel, Spectrochim. Acta 15, 557 (1959).

¹³ L. Genzel, K. F. Renk, and R. Weber, Phys. Status Solidi 12, 639 (1965).

¹⁴ R. J. Elliott, W. Hayes, G. D. Jones, H. F. Macdonald, and C. T. Sennett, Proc. Roy. Soc. (London) A289, 1 (1965).

the H^- ion is anharmonically coupled with its nearest neighbors in the direction of vibration.¹⁵

To summarize, we can say that there can be a sideband structure superposed on a vibrational (or electronic) absorption band of a substitutional impurity in an alkali-halide crystal representing the phonon frequency distribution, possibly multiplied by a frequency-dependent weight function.

IV. LOCALIZED VIBRATIONS

We have shown in the previous section that combination bands of an internal vibration with lattice vibrations of the matrix are rather easily realizable.

In Sec. V we shall present more evidence that the broad sideband structure observed in the nitrate absorption spectrum is indeed related to the phonon frequency distribution of the alkali halide. In the bromides and iodides, however, a number of sharp bands were observed in the frequency regions where the phonon spectrum shows a gap.

Similar bands have been observed in the far infrared spectra.¹⁶⁻¹⁸

The position of the peaks and their small half-width induced us to the assignment to localized vibrations of the impurity ion.¹⁹

It has also been assumed by some authors^{6,20,21} that these bands are due to librations, but no *a priori* calculations have been carried out as yet to check this theory.

A relatively simple approach to the calculation of local mode frequencies has been given by Sievers, Maradudin, and Jaswal.²² We have applied this theory, assuming that one of the halide ions of our matrix is replaced by an ion that differs from the original ion in mass only, and that leaves all force constants unchanged.

Using this isotopic substitution model, the movements of the impurity ion can be described under the point group O_h . Then, the only existing vibrational motion of the impurity transforms like the threefold degenerate representation F_{1u} .

The theory now predicts a local mode of frequency x , when the equation

$$1/\epsilon = x^2 A(x) \quad (1)$$

¹⁵ T. Timusk and M. V. Klein, Phys. Rev. **141**, 664 (1966).

¹⁶ K. F. Renk, Phys. Letters **14**, 281 (1956); **20**, 137 (1966).

¹⁷ C. D. Lytle and A. J. Sievers, Bull. Am. Phys. Soc. **10**, 616 (1965).

¹⁸ A. J. Sievers and C. D. Lytle, Phys. Letters **14**, 271 (1965).

¹⁹ R. Metselaar and J. van der Elsken, Phys. Rev. Letters **16**, 349 (1966).

²⁰ H. Bilz, K. F. Renk, and K. H. Timmesfeld, Solid State Commun. **3**, 223 (1965).

²¹ W. D. Seward and V. Narayanamurti, Phys. Rev. **148**, 463 (1966).

²² A. J. Sievers, A. A. Maradudin, and S. S. Jaswal, Phys. Rev. **138**, 272A (1965).

TABLE VI. Values of the maximum frequencies σ_L (cm^{-1}) for the alkali halides according to the deformation dipole model. Boundaries (cm^{-1}) of the frequency gap between the acoustic and optical phonon branches as found from the near-infrared spectra (this work), from shell-model calculations based on neutron-scattering experiments^a and from deformation-dipole-model calculations.^b

	Maximum frequency	Gap exptl. infrared	Gap shell model	Gap dd model
KI	135.2	69-90	70-96	64-82
KBr	162.0	90-95	90-92	no gap
KCl	210.1	no gap		no gap
NaI	195.0	82-110	77-117	72-95
NaBr	220.2	90-130		100-110
NaCl	258.5	no gap		no gap

^a References 27 and 28.

^b Reference 10.

is satisfied. Here the dimensionless frequency x is defined by $x = \sigma/\sigma_L$, σ_L being the maximum frequency of the crystal (in cm^{-1}). ϵ is a mass-defect parameter, according to the definition

$$M' = (1 - \epsilon)M,$$

M = mass of the original halide ion; and M' = mass of the impurity ion.

The function $A(x)$, which is related to the Green's function of the alkali-halide matrix, is defined by

$$A(x) = (3N)^{-1}P \sum_{\mathbf{k},j} |W(\kappa, \mathbf{k}j)|^2 / [x^2 - \lambda_j^2(\mathbf{k})]; \quad (2)$$

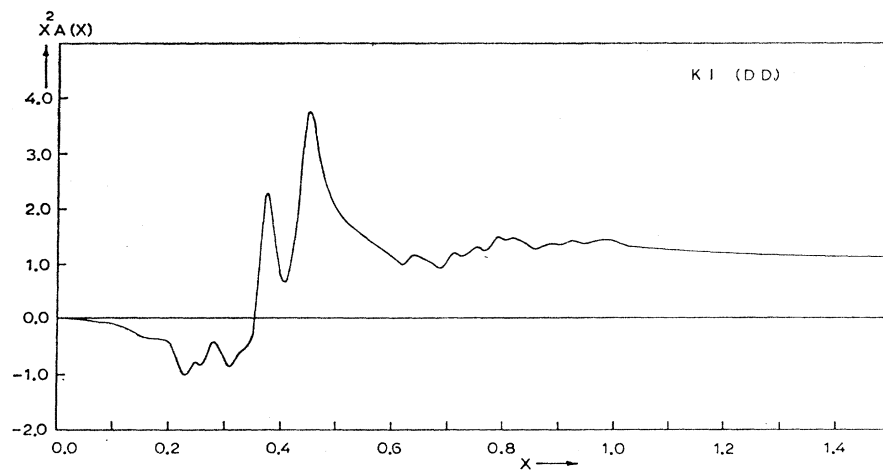
N = number of points in the first Brillouin zone, $w(\kappa, \mathbf{k}j)$ = eigenvector for the κ th kind of ion, associated with an eigenvalue $\lambda_j(\mathbf{k})$, where \mathbf{k} denotes the phonon wave vector and j the phonon branch. P denotes the Cauchy principal value.

The method of solving this equation has been discussed elsewhere.²²⁻²⁴ We evaluated the function $x^2 A(x)$ for the halide ions using the Hilbert transform method. The values of the eigenvectors and eigenvalues employed here, were those calculated by Karo and Hardy¹⁰ from their "Deformation Dipole Model" with 1000 points in the first Brillouin zone.

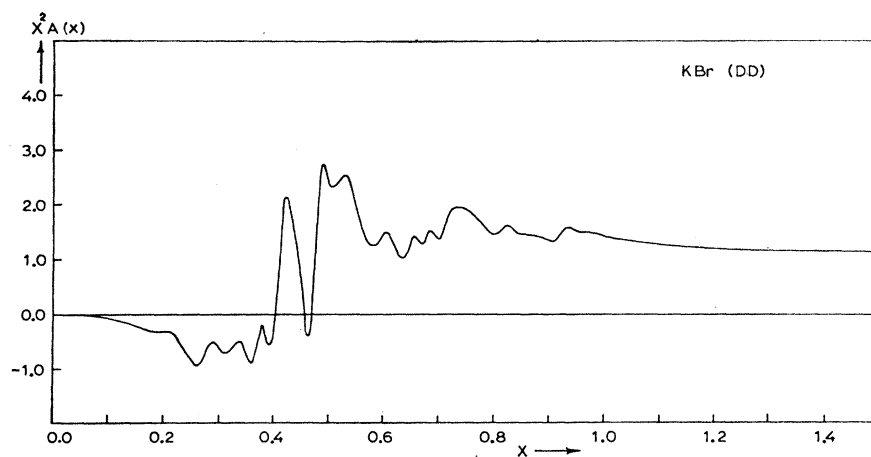
The solutions of Eq. (1) are now easily obtained from a plot of the function $x^2 A(x)$ versus x . The intersections of this curve with a horizontal line drawn at a height of $1/\epsilon$ give the local mode frequencies. The frequencies are found in wave number units after multiplication of x by the maximum frequency σ_L for the lattice, as given in Table VI. The results for six of the alkali halides are shown in Fig. 5.

²³ A. A. Maradudin, E. W. Montroll, and G. H. Weiss, Solid State Phys. Suppl. **3**, 129 (1963).

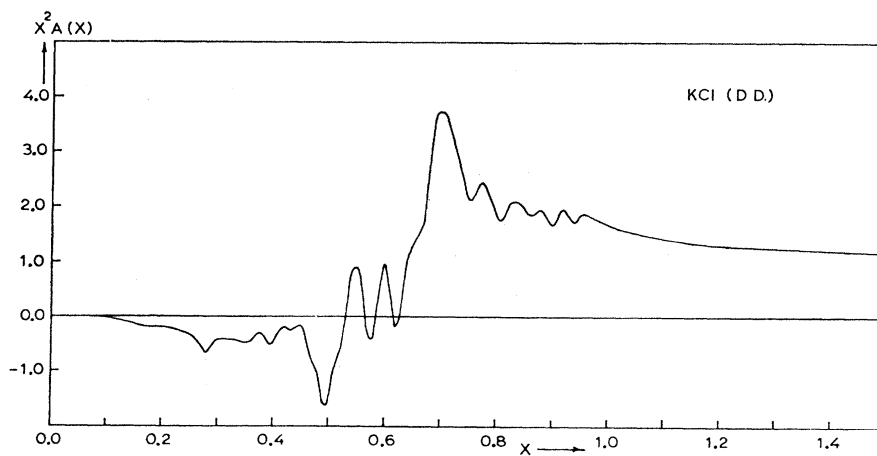
²⁴ R. Metselaar, dissertation, University of Amsterdam, 1967 (unpublished).



(a)

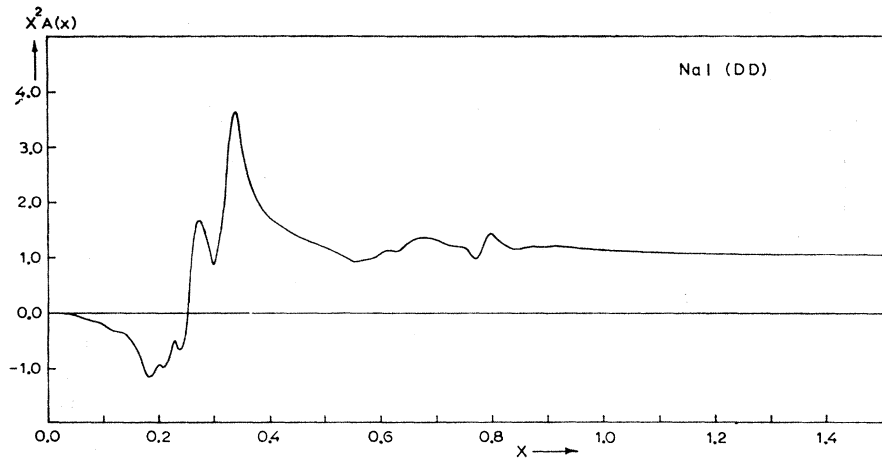


(b)

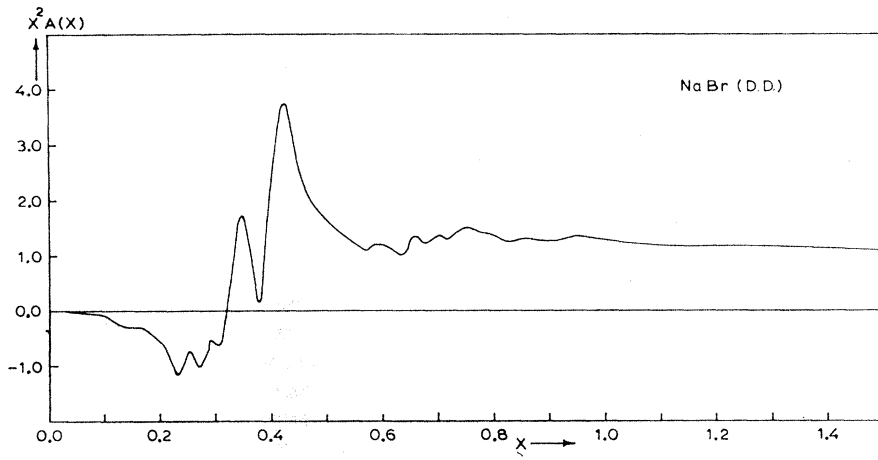


(c)

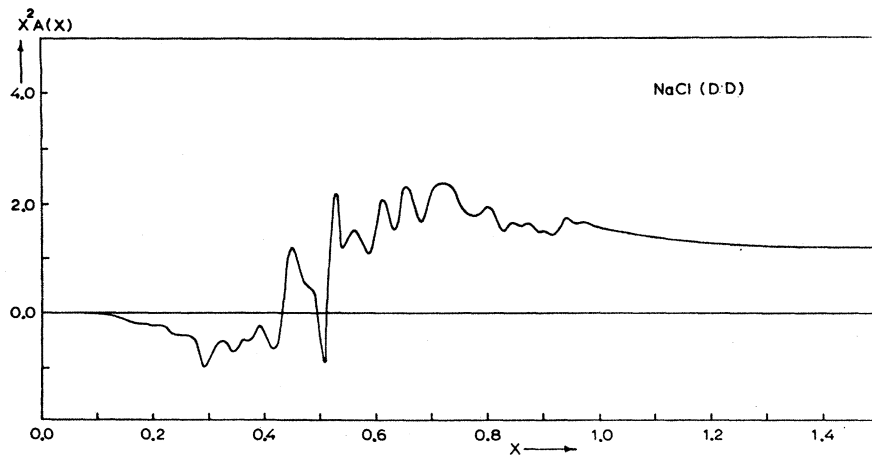
FIG. 5. A plot of the functions $x^2 A(x)$ for the negative ions in the alkali halides. The intersections of the curve with a horizontal line drawn at a height of $(1/\epsilon) = M/(M-M')$ give the frequencies of the localized and resonance modes which can occur when an impurity of mass M' replaces one of the halide ions of mass M .



(d)



(e)



(f)

FIG. 5. (Continued).

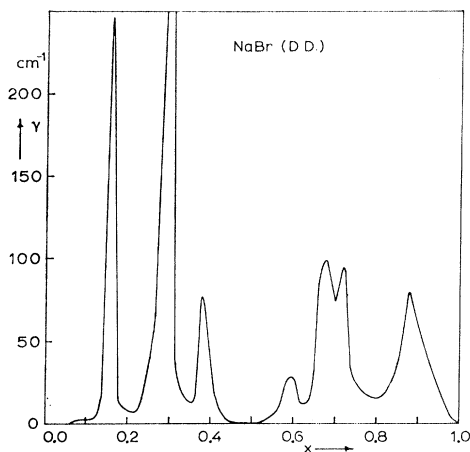


FIG. 6. The linewidth γ of a resonance mode of a negative impurity ion in NaBr as a function of its frequency.

It is of interest to compare our results for KI with those of Ref. 22. The over-all agreement between the curves is satisfactory, but there are some quantitative differences for certain values of x . The differences are probably due to the fact that we used a sample of only 1000 points in the first Brillouin zone, against 5000 points used by Sievers *et al.*^{22,25}

From Fig. 5, together with the data given in column three of Table VI, it is obvious that the solutions of Eq. (1) will not generally be restricted to the region of the frequency gap between the acoustic and optical branches or above the optical branches, but do likewise exist in regions in between. The corresponding modes are called resonance modes. In the harmonic approximation the gap modes cannot exchange energy with the other normal vibrations of the crystal; that is, the corresponding absorption bands have zero bandwidths. The resonance modes, however, being situated in the band of allowed frequencies, will have a finite bandwidth even in the harmonic approximation.

For an estimate of the width γ at half the height of the resonance modes, we used the quantitative expression given in Refs. 22, 26.

We have shown only the result for NaBr here (Fig. 6). Apart from the gap region where $\gamma=0$, the bandwidths are always large (>20 cm⁻¹). An analogous behavior is found for the remaining alkali halides.

So far this theory, as outlined here, has been applied successfully to the far-infrared spectra of Cl⁻ ions in KI.²² To see if the qualitative aspects of the spectra of nitrate and other complex ions dissolved in the alkali halides can also be understood in terms of local-

ized modes of the impurity, we shall discuss a number of examples in the last section. Several objections can be raised against the use of the isotopic substitution model for the complex ions. One of the major disadvantages is the fact that, because of the assumption of a spherical mass point, only one threefold degenerate local mode is predicted. Since most of the complex ions which are to be considered here are by no means spherical ions, we can expect a splitting of the resulting absorption band. The number of components and their infrared activity can easily be predicted if the local symmetry around the ion is known.

A number of improved calculations, including changes in nearest-neighbor repulsive forces, is being carried out in our laboratory.

An effect which can scarcely be taken into consideration in this theory is a possible relaxation of the matrix around the impurity. Such a relaxation is expected to be important when very small or very large ions are substituted in the alkali halides.

V. INTERPRETATION OF THE SPECTRA

A. Frequency Distributions

We showed that combinations of an internal vibration of the impurity ion with lattice vibrations of the matrix may lead to absorption of electric-dipole radiation. Owing to the nearly continuous distributions of the lattice eigenfrequencies, broad absorption bands are to be expected in this case.

For the alkali halides, as yet, there have been no direct observations reported of phonon-frequency-distribution curves. We are forced therefore to compare our experimental results with calculated frequency-distribution curves. For example, we consider the spectrum of KNO₃ in KI (Fig. 3). On the high-frequency side of the ν_3 vibration band of NO₃⁻, we observe, apart from $2\nu_4$, a broad structure with two sharp bands at 75 and 87 cm⁻¹ from the ν_3 frequency. One may hope to get more information from this spectrum, if the absorption contribution of the ν_3 and $2\nu_4$ bands can be eliminated. For this purpose the line shapes of these bands should be known. We have assumed a Lorentz form, though deviations in the wings are known to occur with this band form. At 77°K, the temperature at which the spectra were taken, there is also a contribution of the very broad ν_1 of NO₂⁻. In Fig. 3 we have indicated the estimated total contribution of the NO₂⁻ ν_1 and the NO₃⁻ ν_3 and $2\nu_4$ to the observed spectra. We realize that no high accuracy can be claimed and consequently the contributions to the low-frequency part (0–50 cm⁻¹) of the sideband structure are rather uncertain.

The spectra for five alkali halides, obtained after subtraction of the contributions of the internal vibra-

²⁵ Dr. A. A. Maradudin informed us that similar deviations were obtained in a recent calculation by Dr. G. Benedek, also using 1000 points, but with a different arithmetic method.

²⁶ Because of a printing error, the original expression contains a factor x^2 instead of x .

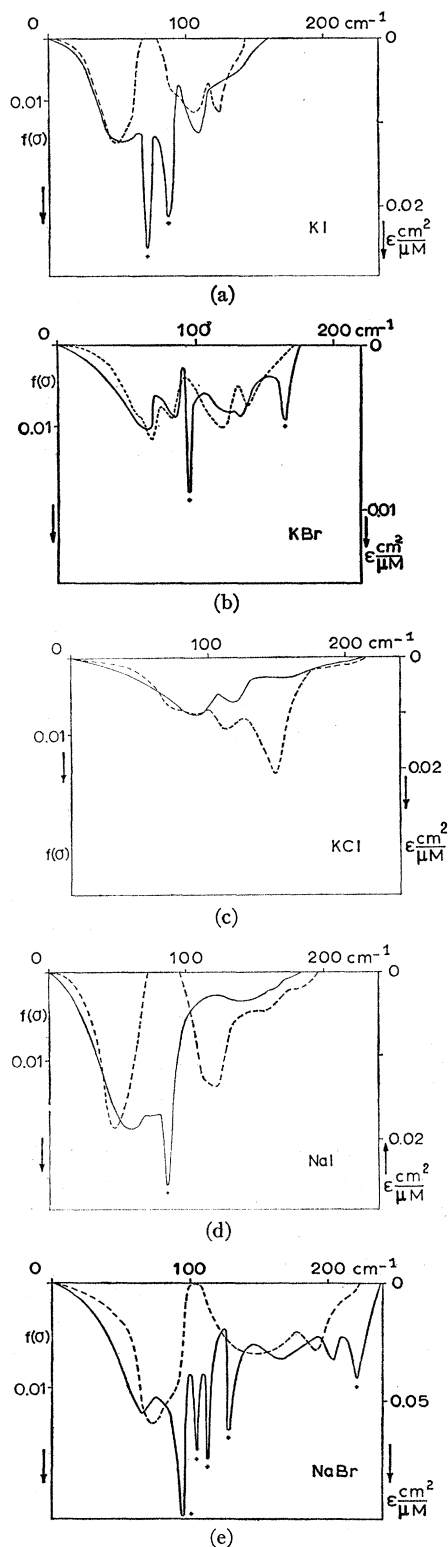


FIG. 7. Additional absorption intensity at 77°K on the high-frequency side of the nitrate ν_3 fundamental (solid line), compared with the calculated phonon frequency distributions, deformation dipole model (Ref. 10), (dashed line). Frequencies relative to ν_3 .

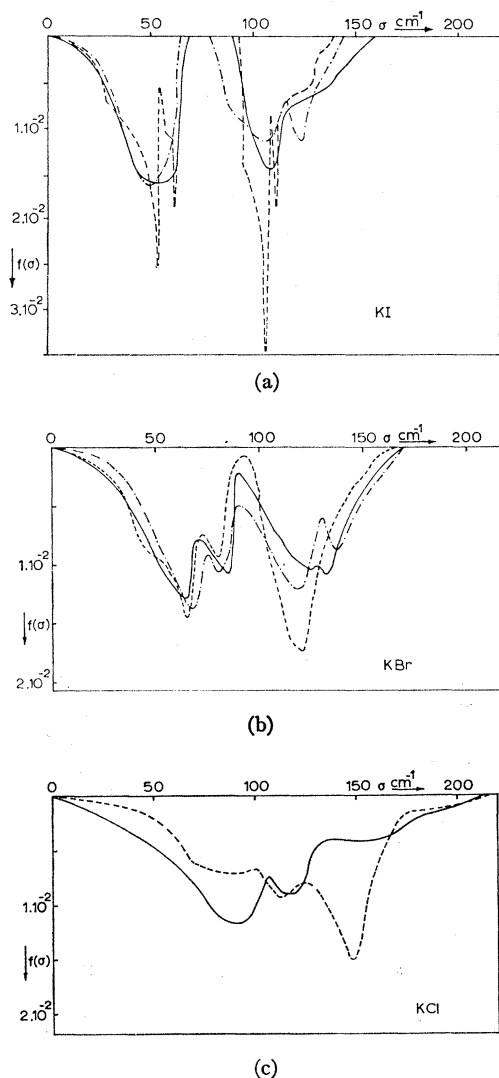


FIG. 8. — Experimental frequency distributions for three alkali halides obtained from Fig. 7 after subtraction of the sharp absorption bands and subsequent normalization. ---. Distribution curve calculated from the deformation dipole model results (see Ref. 10). -.-.- Distribution curve calculated from the shell model results (see Refs. 27, 28).

tions, are given in Fig. 7, together with the theoretical one-phonon frequency-distribution curves calculated from the deformation dipole model.¹⁰ The absorption curves in these pictures are conveniently scaled so that a comparison of the frequencies of the maxima in the absorption curves with those of the frequency distributions can be made. We now see that the maxima of the broad bands in our spectra are found close to the maxima of the theoretical distribution curves. Therefore, we conclude that the broad absorption bands are due to combinations of the ν_3 vibration of the nitrate ion and the lattice vibrations of the alkali halide host lattice. In this way the infrared spectra of complex

TABLE VII. Heat capacities for the alkali halides. (I) Experimental data,^a (II) calculated from the experimental frequency distribution curves (this work) and (III) calculated from the Deformation Dipole model.^b

$T(^{\circ}\text{K})$	KI			KBr			KCl		
	I	II	III	I	II	III	I	II	III
20	2.71	2.92	2.93	1.60	1.99	1.78	0.71	2.04	0.78
30	4.79	4.96	5.12	3.51	3.96	3.86	1.99	4.52	2.23
40	6.33	6.55	6.83	5.30	5.64	5.71	3.56	4.98	3.93
50	7.81	7.72	8.08	6.76	7.02	7.15	5.05	6.39	5.46
60	8.75	8.66	8.97	7.87	8.05	8.20	6.31	7.54	6.72
70	9.43	9.33	9.60	8.73	8.75	8.97	7.35	8.54	7.69
80	9.91	9.86	10.07	9.33	9.33	9.54	8.16	9.04	8.45
90	10.28	10.24	10.41	9.80	9.78	9.97	8.79	9.47	9.04
100	10.57	10.50	10.67	10.15	10.10	10.30	9.31	9.91	9.50
120	10.95	10.90	11.02	10.68	10.56	10.75	10.06	10.45	10.15
140	11.22	11.05	11.25	11.02	10.82	11.04	10.52	10.96	10.58
200	11.59	11.51	11.58	11.54	11.38	11.48	11.24	11.44	11.23
260	11.79	11.78	11.72	11.80	11.54	11.66	11.56	11.64	11.51

^a Reference 29.^b Reference 10.

ions supply valuable experimental information on the lattice dynamics of the matrix. This is especially important since the theoretical-distribution curves are known to be only poor approximations. Not only the positions, but also the number of maxima in the theoretical curves, depend strongly on the potential-energy model used. This is demonstrated in Fig. 8 for KBr and KI, where two curves are presented, calculated from different models.^{10,27,28} Next we will try to verify the quantitative accuracy of the experimental curves. This actually means that we determine the weight factor with which our curves have to be multiplied to represent the true frequency distributions.

The accuracy of a frequency distribution can be checked by calculating the specific heat from the distribution and by comparing this with the available experimental values. This calculation is only possible if we do not count the sharp peaks in our spectra, which are apparently of a different nature.

We first plotted the absorption against the frequency σ . The sharp bands were subtracted by assuming a symmetrical band shape of Lorentzian form. The area under the resulting curve was determined by means of a planimeter. After normalization to unity according to the equation

$$\int_0^{\sigma L} f(\sigma) d\sigma = 1, \quad (3)$$

we obtained the $f(\sigma)$ curves as shown in Fig. 8. In this figure we also indicated the theoretical frequency distribution on the same scale. For the temperature

region 10–300°K the specific heat at constant volume was calculated from the observed distributions using the relation

$$c_v = 6Nk \int_0^{\sigma L} \left(\frac{hc\sigma}{2kT} \right)^2 f(\sigma) \operatorname{csch}^2 \left(\frac{hc\sigma}{2kT} \right) d\sigma. \quad (4)$$

In Table VII our results for the potassium halides are compared with the known calorimetrically determined values²⁹ and with the values calculated from the deformation dipole model.¹⁰ The data from this table are also shown in Fig. 9. Another commonly used check is obtained by comparing the Debye temperatures Θ_D .

In Fig. 10 the Debye temperatures obtained from our spectra are compared with those determined from the experimental specific heat values²⁹ and those calculated from the deformation dipole (dd) model.¹⁰

In general, the agreement between the different c_v and Θ_D values can be called satisfactory, though there are exceptions to be discussed. The deviations at low temperatures are probably due to the uncertainties in our curves at low frequencies. In fact, this part of our curves is hidden under the ν_3 and $2\nu_4$ absorption bands of the nitrate ion. Since only the lowest frequencies play a part in the determination of c_v at low temperatures [due to the factor $\operatorname{csch}^2(hc\sigma/2kT)$], the discrepancies in c_v and Θ_D are expected to be large.

The agreement for KCl is not as good as for KBr and KI. Comparison with the calculated distribution curve for KCl (cf., Fig. 8), shows that maxima occur at nearly the same frequencies; there is, however, a large intensity difference on the high-frequency side.

²⁷ R. A. Cowley, W. Cochran, B. N. Brockhouse, and A. D. B. Woods, Phys. Rev. **131**, 1030 (1963).

²⁸ G. Dolling, R. A. Cowley, C. Schittenhelm, and I. M. Thorson, Phys. Rev. **147**, 577 (1966).

²⁹ W. T. Berg and J. A. Morrison, Proc. Roy. Soc. (London) **A242**, 467 (1957).

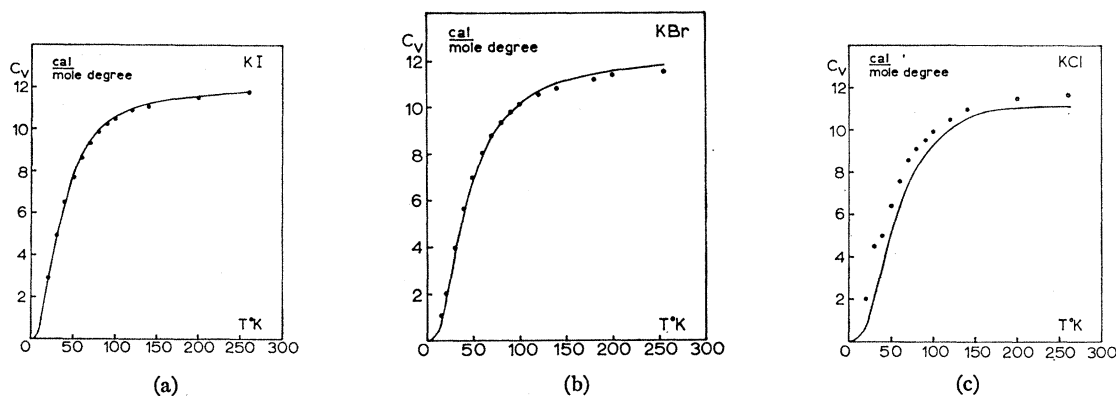


FIG. 9. The specific heat at constant volume of the potassium halides at different temperatures, solid line: experimental values (see Ref. 29), points calculated from the experimental frequency distributions as shown in Fig. 8.

The results for KBr also show that the differences are found mainly for the lowest and highest frequencies. For KI the results are in excellent agreement with the experimental c_v values.²⁹ Comparing the calorimetric values of c_v with the values calculated from the dd model frequency distribution and with those calculated from our experimental distribution function, we find that a much better result is obtained in the latter case. The main differences from the dd model curve are found near the high-frequency side of the optical branches. Our curve agrees rather well with that of Dolling *et al.*²⁸ These authors recently published the results obtained from an accurate model calculation with parameters which were adjusted to give an optimal representation of their experimentally determined eigenfrequencies. The sharp peaks, which they predicted in the acoustic and optical branches, are not resolved in our spectra.

Of the sodium halides, NaCl showed one broad band with a maximum near 35 cm^{-1} . However, in this case, the results are unreliable because of the formation of clusters of nitrate ions.

In NaBr the frequencies of the maxima roughly correspond with those of the maxima in the dd model frequency distribution, but the exact band form is obscured by the many sharp peaks near the frequency gap at the top of the optical branches.

For NaI the frequencies of the maxima again correspond with the calculated frequencies.

The intensity distribution shows large deviations for the optical branches in the case of KCl. One can, of course, assume a varying weight factor to account for the deviations in our distribution curves, but this would be in contradiction with the results obtained on KBr and KI. It is also possible, however, that the deviations in the distributions of KCl and NaI are only trivial. If the contribution of the nitrate ν_3 and $2\nu_4$ absorptions is larger than we assumed, the resulting distribution curve would be lower in the low-frequency region and, because of the normalization, there would be an increase in the high-frequency region.

Generally, we conclude that the broad bands observed on the high-frequency side of the ν_3 fundamental of nitrate ions in an alkali halide represent the maxima in the distribution function of the lattice frequencies. No relation can be given determining the weight of the frequencies in this distribution.

In the last section we also discuss the results obtained by several investigators on the far-infrared spectra of impurity ions in alkali halides. These experiments likewise support the above mentioned conclusions.

Finally, we note that there are other physically interesting data to be found from our spectra, viz., the frequencies of the gap between the acoustic and optical

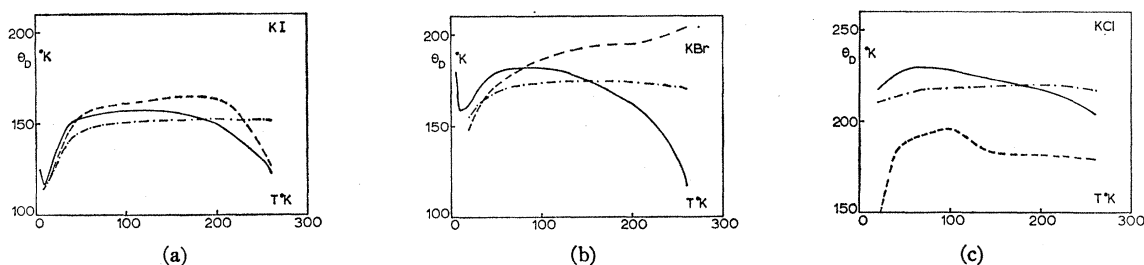


FIG. 10. Debye temperatures as functions of temperature for the potassium halides. — experimental values (See Ref. 29). - - - calculated values (this work) - - - - calculated, deformation dipole model (see Ref. 10).

TABLE VIII. Comparison of calculated and observed frequencies (cm^{-1}) of resonance and gap modes of some impurity ions in different alkali halides.

Investigators	Source	Reference		Gaps and gap modes	
This work	calc. dd		Gap in KI	64-82	
This work	expt. near infrared		Gap in KI	69-90	
This work	calc. dd		NO_3^- , 50, 52, 58	68.5	
This work	expt. near infrared		NO_3^-	73, 87	
Narayanamurti c.s.	expt. near infrared	6	NO_3^-	73, 88	
Cundill, Sherman	expt. near infrared	30	NO_3^-	74, 89	182
Renk	expt. far infrared	16	NO_3^-	72.8, 88, 89	
Lytle, Sievers	expt. far infrared	17	NO_3^-	73.3, 88	
This work	calc. dd		NO_2^- , 50, 58	73	
Narayanamurti c.s.	expt. near infrared	6	NO_2^- , 53, 63	71, 79, 80.5	137, 206
Renk	expt. far infrared	16	NO_2^- , 55, 65	71.1, 78, 79.4	
Sievers, Lytle	expt. far infrared	17, 18	NO_2^- , 55, 63	71.2, 78.4, 79.5	
Timusk, Staude	expt. ultraviolet	31	NO_2^- , 63.5	70	136, 206
This work	calc. dd		CN^- , 49, 53, 57	78	104, 116
Seward c.s.	expt. near infrared	21	CN^- , 43, 60, 68	83	
Lytle, Sievers	expt. far infrared	Unpublished	CN^- , (35-70)	81.5	
This work	calc. dd		OH^- , 49, 53, 57	81	
Renk	expt. far infrared	a	OH^- , 63.7, 69.5	77, 86, 87, 88	
This work	calc. dd		Gap in NaI	72-95	
This work	expt. near infrared		Gap in NaI	82-110	
This work	calc. dd		NO_3^- , 62	75	
This work	expt. near infrared		NO_3^-	86	
This work	calc. dd		NO_2^- , 52, 55, 62	82	
Lytle, Sievers	expt. far infrared	17	NO_2^- , 72	83.8, 93.9	
This work	calc. dd		CN^- , 51, 56, 61	94	130, 155
Cundill, Sherman	expt. near infrared	30	CN^-	93	126
This work	calc. dd		NCO^- , 52, 55, 62	84	
Decius c.s.	expt. near infrared	b	NCO^-	91, 105	
This work	calc. dd		Gap in KBr	None	
This work	expt. near infrared		Gap in KBr	90-95	
This work	calc. dd		NO_3^-	None	
This work	expt. near infrared		NO_3^-	95	165
Cundill, Sherman	expt. near infrared	30	NO_3^-	93	103, 175
This work	calc. dd		Gap in NaBr	100-110	
This work	expt. near infrared		Gap in NaBr	90-130	
This work	calc. dd		NO_3^-	None	
This work	expt. near infrared		NO_3^-	95, 105, 113, 128	221

^a K. F. Renk, Phys. Letters 20, 137 (1966).

^b J. C. Decitus, J. L. Jacobson, W. F. Sherman, and G. R. Wilkinson, J. Chem. Phys. 43, 2180 (1965).

branches. For KI a well-defined frequency gap was found, extending from 69 to 90 cm^{-1} . Therefore, the gap is much larger than calculated from the dd model (64-82 cm^{-1}). Our results were confirmed by the neutron-scattering experiments,²⁹ which produce as result 70-96 cm^{-1} . For NaI we found a gap from 82-110 cm^{-1} , where the dd calculations predicted 72-95 cm^{-1} for the frequency gap. For KBr a gap of only a few wave numbers seems to be present at about 90 cm^{-1} ,

in good agreement with the neutron-scattering results.²⁸ For NaBr, assuming that all four sharp bands, observed near 100 cm^{-1} , are situated in the gap, the gap boundaries will be about 90 and 130 cm^{-1} . No gap was found for KCl and NaCl, in accordance with the theory.¹⁰ The results are summarized in Table VI.

We found that the spectra did not change much from liquid-helium temperature up to about 90°K. This can be explained if only binary combinations

(phonon) + (internal) play a part. At higher temperatures, where evidently multiphonon processes are involved, the bands broaden to one structureless absorption. The difference bands (internal) - (phonon) which fall in the region of the strong nitrite absorption bands have not been observed. At high temperatures the nitrite absorption makes the observation impossible; at low temperatures the intensity will be too low, because of the exponential decrease with temperature.

B. Localized Modes

Apart from the broad bands, our spectra show a number of sharp peaks. Though the frequency gap for the alkali bromides and iodides is not accurately known in all cases, these sharp bands are undoubtedly situated in the gap or in the immediate vicinity of the gap. For the bromides there are also some bands just above the maximum frequency of the optical branches. These facts suggest that the absorption bands may be due to local vibrations of the impurity ion. For this reason we developed the theory for the calculation of local mode frequencies in the alkali halides.

Since the impurity, in our approximation, is only characterized by its mass, solutions can easily be obtained for a wide variety of impurity ions. Apart from our own experimental results on NO_3^- ions, we will therefore also discuss the results obtained by several investigators on a number of different impurity ions. It will be shown that the theory gives a satisfactory explanation of the widely differing experiments, in this way supporting the assumption that localized vibrational modes are being observed in these cases. A survey of the results of our calculations, together with the available experimental data, is given in Table VIII.

First, we shall discuss the spectra found in potassium iodide in detail. The gap is experimentally found between 70 and 96 cm^{-1} , whereas the dd model predicts a gap between 64 and 82 cm^{-1} . For ease of reference the region of the gap for KI is given in Fig. 11 (dd results). The values of the mass parameter $1/\epsilon$ for a number of impurities in KI are shown on the abscissa in this figure, and the frequencies of the resulting gap modes from the definition $\sigma = \sigma_L x$ on the ordinate. The maximum frequency of KI is $\sigma_L = 135 \text{ cm}^{-1}$, according to the dd calculations. As we have seen from our calculations (Fig. 5) there are also solutions in other frequency regions. Since in these cases the phonon density is nonzero, we will designate these solutions as resonance modes. In Table VIII the results of the calculations for KI are compared with the experimentally determined values.

Concerning the nitrate ion it is seen from the table that several authors did also find the two frequencies in the near infrared as combination bands, and in the far infrared as separately occurring peaks. Two noticeable aberrations are the splitting in the 88 cm^{-1} peak as reported by Renk, and the peak at 182 cm^{-1} men-

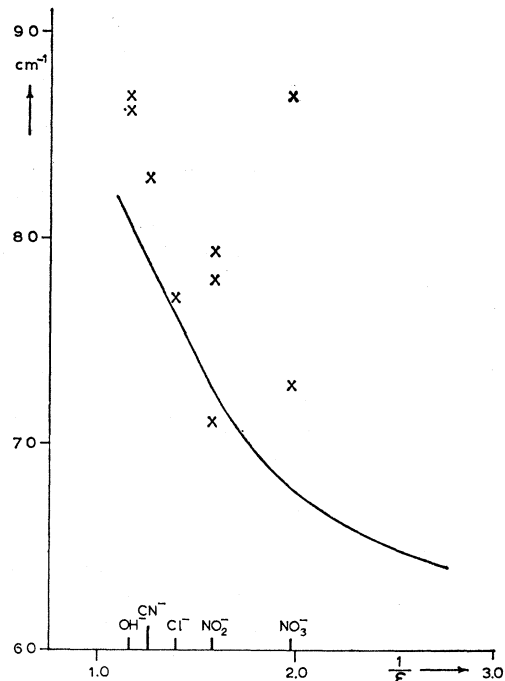


Fig. 11. Frequencies of gap modes for a negative impurity ion in KI as a function of the mass parameter $1/\epsilon = M/(M - M')$. The experimental values are indicated for a number of ions. The line is calculated according to the deformation dipole model (Ref. 10).

tioned by Cundill *et al.*³⁰ In comparing the experimental with the calculated frequencies, it should be realized that the eigenfrequencies calculated from the dd model do not give a sufficiently accurate prediction of the frequency gap. The frequency of the gap modes will suffer the same inaccuracy but the values of the gap mode frequencies relative to the limiting frequencies of the gap are more significant. However, even taking this into consideration, the splitting of the one predicted local mode into two frequencies should be accounted for. The molecular symmetry group is D_{3h} , the local symmetry group probably C_{3v} . Under both symmetry groups the threefold degeneracy of the gap mode will be removed, resulting in one nondegenerate and one twofold degenerate mode. For an orientation of the nitrate ions with the threefold axis along the cube diagonal the A component (parallel to the C axis) will in all probability have the lowest energy. We therefore assign the 73 cm^{-1} band to the A component and the 87 cm^{-1} band to the E component of the gap mode. The predicted resonance modes, one narrow (14 cm^{-1}) near the top of the acoustic branches and two broad (100 cm^{-1}) near 50 cm^{-1} , are not found experimentally. In more accurate dd calculations²² these do not appear either. The origin of the band at 182 cm^{-1} , observed by Cundhill and Sherman, is uncertain. We do not expect a local mode in this region. The first

³⁰ M. A. Cundill and W. F. Sherman, Phys. Rev. Letters 16, 570 (1966).

overtone of the gap mode is allowed under C_{3v} , but the observed frequency is rather high. For the nitrite ion in KI several authors have observed two sharp bands at about 71 and 79 cm^{-1} , together with various weaker and broader absorptions. The results obtained from combination bands or from the far-infrared spectra are about the same. Measurements in the ultraviolet³¹ showed one sharp band at 70 cm^{-1} in combination with the vibronic band in which the totally symmetric bending vibration was singly excited. Our calculations predict one gap mode at 73 cm^{-1} , whereas a resonance mode might possibly be present at 58 cm^{-1} . For an orientation of the nitrite ion with the twofold axis along the $[110]$ axis of the crystal,⁶ the local symmetry group would be C_{2v} and the threefold degenerate gap mode would split in the species $A_1+B_1+B_2$. All three components are allowed in a direct transition. In combination with the ν_3 (B_1) vibration only two components, viz., A_1 and B_1 , are allowed. The selection rules for the ultraviolet spectrum cannot be derived in the same direct way. The selection rules for this case of vibronic coupling were derived by Bron and Wagner.³² Under C_{2v} symmetry the 1B_2 electronic state of the nitrite ion can couple with A_1 modes. As only one band at 70 cm^{-1} is observed in the ultraviolet spectrum, we assign this band to the A_1 component of the gap mode. Assuming that the frequency of this mode would not be very different for combinations with the ground state or the first excited state, we assign the frequency of 71 cm^{-1} as found in the infrared to this same mode. The bands at 79 cm^{-1} may be the B_1 and B_2 components. If the local symmetry were lowered to C_2 , C_s , or E , a slight energy difference between these two components might be expected. The bands found at higher frequencies are probably the first and second overtones of the gap modes, whereas the bands at 55 and 65 cm^{-1} may very well be due to the maxima in the phonon-distribution curve of KI.

As for the frequencies found in KI with CN^- and OH^- impurities, it seems appropriate to assign the bands found at 83 cm^{-1} in the combination band and at 81.5 cm^{-1} in the far infrared to the one predicted gap mode at 78 cm^{-1} for the cyanide ion. For the hydroxyl ion one gap mode is predicted at 81 cm^{-1} and a sharp resonance mode at 57 cm^{-1} . The OH^- ions are probably directed along the $\langle 100 \rangle$ axes.³³ The local symmetry group is therefore C_{4v} . Hence, a splitting of the gap mode in two active components of species A_1 and E is possible. We assign the strong sharp bands at 86.2 and 86.9 cm^{-1} , respectively, to the A_1 and E components of the gap mode and the band reported at 69.5 cm^{-1} to the resonance mode.

The spectra that have been determined for various impurities in the other alkali halides can be assigned in a similar way as for KI. The results can also be

found in Table VIII. It is easy to indicate the gap modes for sodium iodide. With nitrite and cyanide impurities some broad bands correspond to maxima in the phonon distribution at 50 and 72 cm^{-1} , respectively, at 125 cm^{-1} . According to the theory no gap modes are to be expected in the bromides and in the chlorides. As far as the chlorides are concerned, this is in accordance with the experiments, but the results found with the bromides are in striking contrast to this expectation. In potassium bromide with nitrate impurities there are two sharp bands at 95 and 165 cm^{-1} and in sodium bromide four distinct peaks, which do have the appearance of local modes and are situated in the gap or above the maximum frequency.

VI. DISCUSSION

The material presented in the preceding section clearly shows that we are justified in attributing the broad absorption bands observed on the high-frequency side of the ν_3 fundamental vibration band of nitrate dissolved in an alkali halide, and the sharp bands found in the same frequency region, to different causes.

The supposition that the broad sideband structure represents the phonon distribution of the matrix is confirmed by the observed agreement between the specific-heat values calculated from the spectra and the experimental values of the specific heat. In the far-infrared absorption spectra of NO_3^- , NO_2^- , and CN^- in KI and NaI, which have been reported by other authors, the distribution curves of the alkali halides are not recognizable, but we do find the maxima in this distribution in accordance with the theory. From the distribution curves observed in the near-infrared spectra, we can, moreover, determine the boundaries of the frequency gap, between the acoustic and optical branches, present in the alkali iodides and bromides.

The sharp bands that we observe in the spectra of nitrate ions in the alkali bromides and iodides, are situated either in this gap or above the maximum frequency of the lattice. The same is to be found in the far infrared spectra of several complex ions in these matrices. From this we inferred that the sharp absorption bands must be assigned to the localized vibrations of the complex ions in the host lattice.

The relation between the observed frequencies and the local mode frequencies as predicted by the theory is best illustrated by Fig. 11. The curve drawn in this figure gives the frequencies of the local mode in KI as a function of the mass parameters. This curve is calculated according to the theory as outlined here. It allows for one local mode frequency for each impurity as a consequence of the simple isotopic substitution model used. The dots represent the experimental results. We have included in this figure the gap mode frequency of Cl^- . Actually, this is the only ion having the local symmetry group O_h , as assumed in our model. For the other ions the local symmetry group is lower

³¹ T. Timusk and W. Staude, *Phys. Rev. Letters* **13**, 373 (1964).

³² W. E. Bron and M. Wagner, *Phys. Rev.* **139**, 233 (1965).

³³ U. Kuhn and F. Lüty, *Solid State Commun.* **2**, 281 (1964).

and hence the threefold degeneracy of the localized vibration may be removed. From the figure it is seen that, in accordance with the theory, the frequencies of the observed absorption bands decrease with increasing mass of the impurity ion (increasing mass parameter $1/\epsilon$). At the same time, the figure shows the shortcomings of the calculations. In the first place, all the experimental points are systematically found at higher frequencies than the theory predicts. Since the same applies to the frequencies limiting the gap (see Table VIII), it is probable that the values of the eigenvectors and eigenfrequencies that we used in our model calculations are responsible for this deviation. In the second place, the occurrence of more than one local mode in the spectra of some of the ions violates the theoretical predictions. The observed splittings of the absorption bands indicate that we should at least account for the nearest-neighbor repulsive forces. It is suggestive that the largest deviations, both for splitting and the frequency shifts, occur with the nitrate ion and more particularly with the E component of the gap mode for this ion. This may mean that the nitrate ion, which is the largest of the ions under consideration, causes a perturbation of the lattice. Such a perturbation can certainly be expected where the nitrate ion is dissolved in alkali halides with smaller lattice constants. This may be the reason why the results of theory and experiment do not agree at all for the alkali bromides. Similar conclusions have been made for alkali halides with H^- ions (U -center bands). In these cases the hydrogen ion is so much smaller than the halide ion, that a relaxation of the lattice is probable.

From our data it cannot be decided whether the permanent dipole moment present in a number of these ions influences the frequencies of the local modes. In these cases the long-range forces may be altered too, which can cause a decrease of the degree of localization.

However, more detailed calculations of the defect modes will be feasible only when improved values of the eigenfrequencies and eigenvectors of the pure alkali-halide lattices become available.

Furthermore, it follows from the theory that, apart from the strictly localized modes, vibrations with fre-

quencies in the regions with a finite phonon density are also possible. Because of the interactions of these resonance modes with the lattice modes, they have a finite lifetime even in the harmonic approximation. From our calculation we find in most cases bandwidths of the order of 100 cm^{-1} , which indicates that it will be difficult in general to distinguish these absorption bands from the bands due to the continuum of lattice modes. Our experimental results confirm this presumption. The observed broad bands can be attributed to the phonon frequency distribution of the matrix, without the necessity to assign some bands to resonance modes.

We mentioned that the sharp bands have been ascribed to librations of the complex ions around one or more axes.^{6,20,21} However, in view of the agreement between theory and experiment for a series of complex ions, it is preferable to describe the absorption bands in terms of localized vibrations.

On the other hand, we have to take into consideration that a strong coupling between translations and rotations is possible in many of these cases. This means that the separation of these degrees of freedom in the Hamiltonian is not valid and the use of these names no longer makes any sense.

For a further test of the ideas developed here, it is necessary to improve the calculations based on a more detailed description, including changes in the force constants and relaxation of the host lattice.

A series of measurements of the far-infrared spectra of complex ions in KI, NaBr, and NaI is in progress in our laboratory.

ACKNOWLEDGMENTS

The authors wish to express their gratitude to Prof. Dr. G. J. Hoijsink, University of Sheffield, for his kind support, and to Dr. J. Groeneveld, Institute for Theoretical Physics, University of Amsterdam, for helpful discussions. We are indebted to Dr. A. M. Karo for making available the eigenvectors and eigenvalues. The work described here is part of the research program of the Foundation for Fundamental Research of Matter (F.O.M) and was made possible by financial support from the Netherlands Organization for Pure Research (Z.W.O.).